
Bifunctional polyacrylamide based polymers for the specific binding of hexahistidine tagged proteins on gold surfaces

Lucas B. Thompson, Nathan H. Mack and Ralph G. Nuzzo*

We describe a modified bifunctional analogue of polyacrylamide that spontaneously forms self-assembled polymeric thin films on Au surfaces. The film is engineered to specifically bind histidine tagged proteins (6His), while simultaneously remaining inherently resistant to the non-specific adsorption of proteins in solution. The backbone of a polyacrylamide-co-*n*-acryloxysuccinimide copolymer is functionalized *via* tandem active ester (NHS) couplings with 3-(methylthio)propylamine (MTP) and nitrilotriacetic acid (NTA). The resulting functionalized polymers form stable and exceptionally hydrophilic thin films that are 2–5 nm thick, a mass coverage that varies with the MTP graft density. These films are characterized using a variety of techniques (X-ray photoelectron spectroscopy (XPS), reflection absorption infrared spectroscopy (RAIRS), ellipsometry, surface plasmon resonance (SPR), and matrix assisted laser desorption ionization (MALDI)) to establish their structure and function. The protein resistance of the films, as demonstrated by their exposure to solutions of bovine serum albumin (BSA), can be modulated by the amount of MTP grafted to the polymer, which in turn, affects their mass coverage. We show that it is possible to specifically capture hexahistidine tagged proteins with low incidences of nonspecific adsorption using these materials, a discrimination quantified using surface plasmon resonance (SPR) at concentrations down to 20 nM. These polymers also bind strongly to the surfaces of Au nanoparticles, stabilizing them against aggregation, providing them with a similar capacity to selectively bind 6His tagged proteins that can then be speciated using MALDI.

Introduction

Control of biomolecular interactions occurring at interfaces is an important focus of current research in surface chemistry that has direct implications in many emerging technologies.^{1–5} The ability to tailor a surface such that it will readily bind to a targeted analyte, yet remain highly resistant to nonspecific protein adsorption, is a critical requirement, one that relies, at least in part, on the precise modification of surface interactions.^{6–8} Even with well-defined surface chemistries such as those afforded by self assembled monolayers (SAMs), the elucidation of general design principles for controlling biomolecular surface interactions remains a significant challenge.⁹ These interactions are inherently complex and involve a number of competing forces (electrostatic, hydrophilic/hydrophobic, covalent binding, *etc.*), each contributing to specific forms of high affinity binding and competing forms of nonspecific adsorption.^{10–12} Specific binding interactions typically involve highly specialized molecular recognition components that provide an enhanced degree of selectivity. Systems used extensively in assays include

antibody-antigen, enzyme-protein and protein-protein pairings, metal-based affinity complexes, as well as the ubiquitously exploited pairings of biotin-avidin.^{13–18} Nonspecific binding, which lacks any sort of recognition element and usually involves deleterious protein denaturing at the surface, is a common background that can significantly impact the limits of detection of a sensor in a biomolecular assay. For this reason it is felt that improvements in surface modification chemistries could both extend and enable novel bioassays that have increased sensitivity as well as selectivity.¹⁹ The present work addresses itself to that interest.

One specific interaction that is commonly used to capture and purify expressed recombinant proteins is based on the affinity of oligohistidine segments (6His) for metal ions such as nickel.^{16–18,20–28} In this affinity system, the Ni²⁺ ion has four of its chelating sites occupied by a ligand (nitrilotriacetic acid, NTA) which is typically used to immobilize it on the stationary phase of a chromatography column. The remaining two chelating sites are available to bind to the imidazole ring of the histidine residues on an expressed protein modified to carry the affinity tag. Notably, this interaction is highly specific due to the unique chelating sizes of the NTA and 6His residues with respect to the Ni²⁺ ion. The dissociation constant for the 6His-Ni-NTA complex ($K_d = 10^{-13}$ at a pH of 8.0) is strong enough to essentially irreversibly bind any 6His tagged analyte to the immobile phase, resulting in complete separation from other interfering background proteins.²⁸ This highly specific

Department of Chemistry, University of Illinois at Urbana-Champaign,
600 S. Matthews Ave., Urbana, IL 61801.
E-mail: r-nuzzo@illinois.edu; Tel: 1-217-244-0809

interaction is well suited for controlling the binding of target proteins in a surface-based bioassay.

The sensitivity and selectivity requirements of advanced bioassays necessitate sensor interfaces that have a high degree of uniformity. Self-assembled monolayers (SAMs) offer a facile approach to the modification of surfaces in this way and provide a well-defined starting point from which to perform subsequent modification for specific sensing applications.^{9,29–31} Simple alkyl silane and thiol-based SAMs, however, do not expressly reduce nonspecific adsorption and more highly functionalized analogues are often fouled by competing forms of biomolecular adsorption in a heterogeneous protein solution. One common approach to reduce this nonspecific adsorption background is to functionalize the SAM with highly hydrophilic polyethyleneglycol (PEG) terminal groups.^{5,20,32–36} The close packed 2-d structure of the PEG groups strongly inhibits nonspecific adsorption in simple protein solutions, but are not always as effective in more complex systems.^{29,34,37} Typically these PEG based SAMs are one component of a mixed monolayer system, the other being a SAM with specific binding capabilities. While these types of mixed monolayers have been shown to selectively bind a variety of biomolecules with minimal nonspecific adsorption, alternative schemes based on polymer thin films can yield similar properties and in some cases provide enhancements of stability that are not possible with simpler SAM architectures.^{6,14,15,38,39}

Polymer thin films also present a unique ability to create a more three dimensional surface structure, one that can be tailored to have specific properties based on the chemical nature of the polymer side chain groups.^{38,39} Compared to a SAM, thin films composed of linear polymer chains can adsorb to a surface in numerous configurations such as loops, trains, and tails that extend away from the surface into solution, and for this reason might be expected to display a much more porous film with a larger degree of disorder.⁴⁰ The precise configuration of the linear polymer surface morphology, however, is strongly influenced by the chemical functionality of any polymer side chain functional groups. For example, a polymer chain functionalized with a ligand that has an affinity for a surface will tend to be more tightly bound, creating a denser and less solvent penetrated film. A polymer chain that is cofunctionalized with a ligand that has an affinity for a specific analyte will form a less dense film, but also have the capability to capture analytes in solution. Varying the relative amounts of these two types of ligands is expected to dramatically affect the performance of such films in protein sensing applications, and with proper design could make polymer films of this type attractive as modifiers for a range of different surfaces including those of both planar- and particle-based assays.^{41–44}

Nanoparticle surfaces are an interesting example of the latter and have been used in a diverse set of applications, such as contrast agents for biological imaging, fluorescent markers, colorimetric bioassays, and as capture agents for biomolecules.^{45–50} Metallic nanoparticles offer a platform similar to planar surfaces that may be exploited to control the surface chemistry *via* SAMs and polymer thin films. More specifically gold nanoparticles with diameters of ≈ 15 nm are

particularly useful due to the strong plasmon absorption near 520 nm, which is highly sensitive to the refractive index of the material that directly surrounds the surface. Clusters of this type have been intensively studied and used in many forms to sense surface binding events.^{41,44,51–54} The large surface to volume area of the nanoparticles also make them ideally suited as collecting concentrating vehicles by binding small amounts of analytes such as neuropeptides, which allows for easy manipulation and offline analysis.^{22,49}

In this work, we demonstrate a high molecular weight ($\approx 49\ 000$ g mol⁻¹) polyacrylamide analogue that provides a modified Au surface that is strongly resistant to protein adsorption while still incorporating a specific protein binding moiety in high segmental density. These bifunctional polyacrylamide analogues assemble on the gold surface through sulfur bearing ligands and specifically bind histidine tagged proteins (6His) through an NTA derivative (Scheme 1). This polymer thin film is readily formed on both planar as well as nanoparticle gold surfaces, and can be used to capture and detect proteins using SPR and MALDI-TOF mass spectrometry.

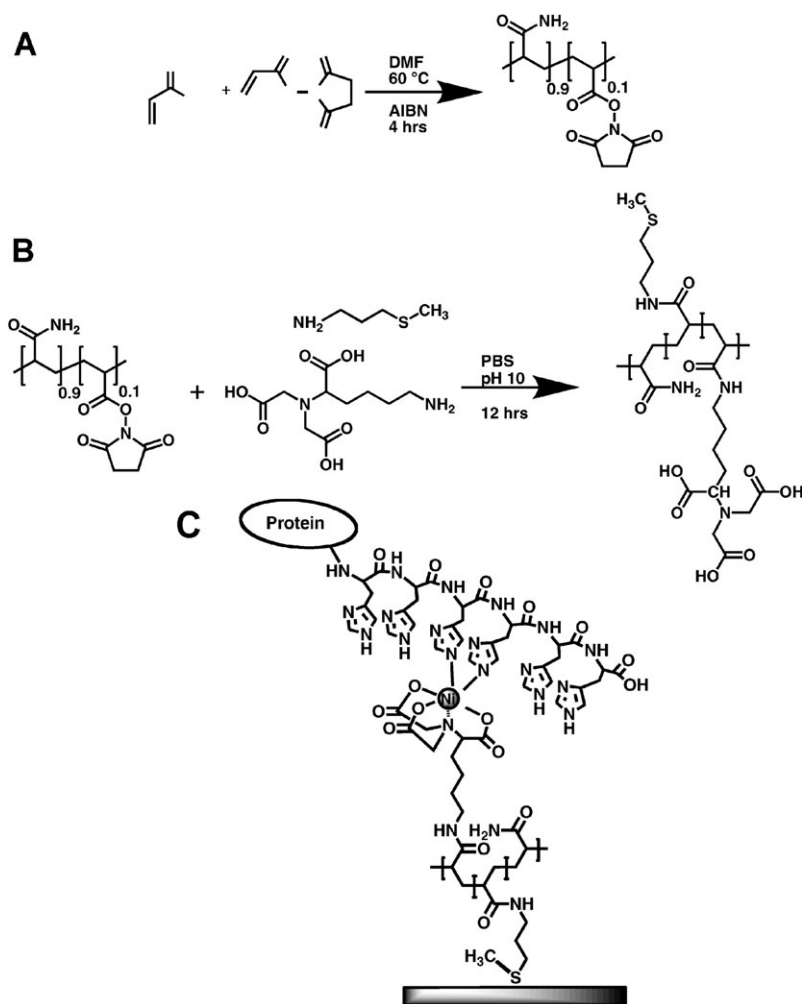
Experimental

Reagents

All reagents were purchased from Sigma Aldrich and used as received unless otherwise stated. Deionized water was generated from a MilliQ Academic A10. 3-(methylthio)propylamine (MTP) was purchased from Acros and used as received. Hexahistidine tagged Ubiquitin (6His-Ub 9600 Da) and human antitrypsin portland (a1-PDX 47 000 Da) proteins were purchased from Calbiochem and used as received.

Polymer synthesis

Polyacrylamide-co-*n*-hydroxysuccinimide (PAN) prepolymer was synthesized by the free radical polymerization of acrylamide and *n*-acryloxysuccinimide as described previously.⁵⁵ Briefly, 4.14 g of acrylamide was added to 800 mg of *n*-acryloxysuccinimide in 65 mL of dimethylformamide (DMF) along with 65 mg of azobisisobutyronitrile (AIBN). The monomer mixture was heated to 60 °C using an oil bath and allowed to react for a period of 2 h. The resulting white precipitate was then rinsed twice with DMF followed by precipitation in ethanol to further purify the polymer. The prepolymer was then modified with an excess of primary amine ligands (MTP and NTA) in 0.1 M phosphate buffer (pH ≈ 10.8). The resulting grafted polymer is hereafter named by the ratio of MTP to NTA in the solution prior to the reaction with the PAN prepolymer. The prepolymer is allowed to react with the primary amine solution for a minimum of 12 h at which point a precipitate is formed by the addition of excess ethanol. The resulting milky solution is concentrated by centrifugation (≈ 2000 rpm for 1 h) and then decanted to remove unreacted ligand and dissolved in MilliQ water. After at least two precipitations the resulting polymer is dried under vacuum for 2 d. To examine the effects of MTP and NTA functionalization, five variants of the functionalized polymer were synthesized and are labeled according to their respective



Scheme 1 General scheme for modifying polyacrylamide-co-*n*-acryloxysuccinimide prepolymer with primary-amine-containing ligands: (A) synthesis of the active ester prepolymer; (B) the reaction of the active ester prepolymer with primary amines; and (C) the binding of a hexahistidine tagged biomolecule through the Ni-NTA complex.

MTP percentage; 100% NTA (PAN-0), 25% MTP to 75% NTA (PAN-25), 50% MTP to 50% NTA (PAN-50), 75% MTP to 25% NTA (PAN-75), and 100% MTP (PAN-100).

Nanoparticle synthesis

Gold nanoparticles were synthesized using the common methods as outlined previously.⁵⁶ Briefly, 34 mg of HauCl_4 was added to 100 mL of H_2O containing 118 mg of sodium citrate which was then brought to reflux for 1 h while constantly stirring. During the reaction the solution goes from a clear yellow color to a dark wine red color. The Au NPs have an average diameter of 14.07 ± 1.1 nm as measured by TEM.

Surface plasmon resonance

The polymer thin films and their relative protein affinities were determined using a home built surface plasmon resonance apparatus in the Kretschmann configuration.⁵⁷ This system uses a p-polarized laser diode (635 nm; 4 mW-Thorlabs) reflected off the back of a gold coated (50 nm) microscope slide onto a silicon photodiode using an index matched equilateral BK-7 (Edmund Optics) glass-coupling prism. The

SPR response was calibrated using a series of increasing concentration ethanol-water solutions with known refractive indices as measured using an Abbe refractometer (Fischer Scientific). This sensitivity factor was used along with an exponentially weighted single layer effective refractive index model to determine the approximate adsorbed polymer film thickness.⁵⁸ The single layer model was extended to include subsequent protein/polymer layers with an assumed refractive index of n_D^{20} 1.46 for all organic layers. SPR experiments determining the total mass coverage of the polymer variants and their relative resistance to non-specific protein adsorption were conducted at a flow rate of 100 mL min^{-1} and held at a constant temperature of $26 \text{ }^\circ\text{C}$. All polymer solutions were at a concentration of 1 mg mL^{-1} with a 30 min adsorption followed by 30 min PBS rinse. Non-specific adsorption of proteins was tested using a 1 mg mL^{-1} solution of BSA for a period of 30 min followed by a 30 min PBS rinse.

To demonstrate the ability of the polymer variants to specifically capture hexahistidine tagged proteins, polymer films composed of PAN-25, PAN-50, and PAN-75 were charged with 100 mM Ni^{2+} and then exposed to varying amounts of 6His tagged proteins. The binding of 6His tagged

proteins was studied using a Biacore 3000 at a flow rate of 5 mL min⁻¹, in HEPES-buffered saline (10 mM HEPES pH 7.6 150 mM NaCl) supplemented with 0.005% P20 surfactant, at a temperature of 25 °C. Prior to any protein injections, a 3 min injection of 0.35 M EDTA solution was exposed to the surface of the sensing chips to remove any metal ion contaminants. The specific binding of the 6His tagged proteins to the surface was preceded by a 25 mL injection of 1 mM Ni²⁺ to charge the NTA followed by a 50 mL injection of protein solution at varying concentrations. For the determination of non-specific binding to the polymer thin films the Ni²⁺ injection was omitted and the protein solutions had 5 mM EDTA added to the protein solution to scavenge any spurious metal ions that may interfere.

X-Ray photoelectron spectroscopy (XPS)

Photoelectron spectra of the polymer thin films were acquired on a Kratos Axis Ultra XPS spectrometer using a monochromatic K α X-ray source with a 40 eV pass energy. The resulting spectra were energy corrected to the Au 4f_{7/2} peak binding energy of 84 eV and baseline corrected by subtracting a linear fit. XPS substrates were prepared by depositing 20 nm of Ti followed by 80 nm of gold on freshly piranha (3 : 1 H₂SO₄ : H₂O₂) cleaned microscope slides. The substrates were then exposed to the 1 mg mL⁻¹ solutions of the polymer variants for a period of 30 min followed by washing with milliQ water.

Reflection-absorption infrared spectroscopy (RAIRS)

An external RAIRS optical bench was used in conjunction with a conventional Fourier transform spectrometer (Bio-Rad FTS-60). The light in the external beam was incident on the sample at a grazing angle of $\approx 85^\circ$. The signal was collected on a liquid nitrogen cooled narrow band MCT detector at a resolution of 1 cm⁻¹ using 512 scans and a 20 kHz modulation. Background scans were collected from freshly cleaned unmodified gold substrates.

Matrix assisted laser desorption ionization (MALDI)

Encapsulated nanoparticles were formed by adding 1 mL of the Au NPs as synthesized to 1 mL of the polymer variants at a concentration of 1 mg mL⁻¹. The NP PAN solution was allowed to react for a minimum of 3 h followed by centrifugation at 13 200 rpm for 1 h to concentrate the NPs and subsequent removal of excess unreacted polymer and resuspension in MilliQ water. After removal of the excess polymer, the solution was split into two equal portions with one portion exposed to a 100 mM Ni(SO₄) solution for 30 min. The NP-polymer solution was centrifuged and resuspended twice in MilliQ water to remove excess Ni²⁺. Both the Ni²⁺ charged Au NP-polymer hybrid and the uncharged Au NP-polymer hybrids were then exposed to 1 mg mL⁻¹ solutions of hexahistidine tagged Ubiquitin (6His-Ub) for 30 min followed by centrifugation and washing three times. Finally, 1 mL of the concentrated Au NP-polymer hybrids was spotted onto a 64 well MALDI target plate along with 1 mL of 10 mg mL⁻¹ sinapinic acid in 60% acetonitrile. All washes and resuspensions were done with MilliQ water. MALDI spectra

were collected on a Bruker UltraflexII in linear mode with a positive bias applied (100 spectra).

Ellipsometry

Ellipsometric measurements were made with a Gaertner Scientific (Chicago, IL) model L116C ellipsometer equipped with a He-Ne laser set at an incidence angle of 70. Measurements were taken at 9 points randomly selected across the surface and averaged. A two-layer transparent film model was used for the thickness calculations based on pseudo-substrate constants measured from a clean substrate. The refractive index of the organic film was fixed at n_D^2 1.46.

Results and discussion

Polyacrylamide-co-*n*-acryloxysuccinimide is a useful material that serves as a versatile platform for creating highly tunable polymer thin films based on the pendant groups attached to the polymer backbone.^{14,55,59} In the present case, we describe a modification of this material that provides bifunctional polymer thin films that are generally resistant to protein adsorption while still binding 6His tagged proteins with high specificity. The two ligands used for this purpose, MTP and NTA, act to promote the rapid formation of a self-assembled thin film through a high affinity for the gold surface as well as impart the ability to bind the analytes respectively. Polymers prepared with varying ratios of MTP to NTA exhibit properties that range from relatively poor protein resists to high quality films for selective binding. The synthetic approach for this PAN prepolymer synthesis results in a linear chain polymer with a MW of $\approx 49\,000$ g mol⁻¹ as determined by static light scattering (Supporting information Fig. S1). With these polymer dimensions, and an initial monomer loading ratio of 10% *n*-acryloxysuccinimide to 90% acrylamide, this results in approximately 60 reactive succinimide side groups per chain that are available to react with amine ligands. The subsequent functionalization by primary amines (MTP and NTA) was followed by monitoring *via* UV-Vis for the presence of free succinimide at 260 nm (ESI, Fig. S2w). No significant differences in the condensation kinetics were observed for the two ligands under the conditions the coupling reactions were carried out, indicating that the final ligand ratios of the functionalized PAN are reflective of the initial ligand ratios in solution.

XPS survey spectra of the polymer thin films show only the presence of carbon, oxygen, and nitrogen with no other elemental contaminants. It is readily apparent from the C1s photoelectron intensities that PAN-0 adsorbs without the assistance of MTP, but an increase in MTP graft density dramatically increases the amount of polymer present on the surface, producing two well resolved peaks at 285.0 eV and 288.0 eV which correspond to the sp³ hydrocarbon backbone of the polymer and the sp² carbonyl carbons (Fig. 1). As the relative amount of MTP is increased to 75%, the C1s peaks increase in intensity; however, further increases in MTP ligation result in a decrease in C1s intensity. This trend is indicative of a film whose mass coverage steadily increases as the MTP content goes from 0 to 75% and then decreases as it is further raised to 100%. Analysis of the nitrogen 2p peak at

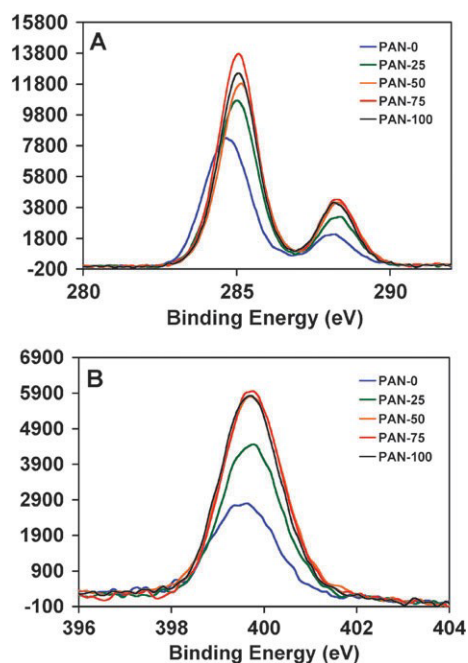


Fig. 1 XPS spectra of (A) C1s and (B) N1s of modified PAN thin films—Black-PAN-100, Red-PAN-75, Orange-PAN-50, Green-PAN-25, Blue-PAN-0.

399.8 eV reveals a similar trend with increasing MTP content. Going from PAN-0 to PAN-25 the N2p peak is nearly doubled in intensity showing that the addition of MTP greatly increases the amount of polymer present on the surface. These data hint at underlying structural changes in the polymer films that are a result of polymer chain modification with MTP ligands. As the MTP graft density increases past 75% it is expected that the surface becomes saturated with polymer, leaving less sites available for additional polymer to bind to the surface resulting in a more compacted surface structure.

To further explore the effect of MTP ligand grafting density, RAIRS was employed to monitor the mass coverage/conformation of chains on the surface (Fig. 2). The RAIRS spectra showed intense absorption features, consistent with the amide I and II bands of the polymer backbone, for all of the polymer variants. The frequency of the stretches remains essentially constant regardless of the relative ratio of the MTP to NTA. As evidenced by the XPS data there is some physisorption of the polymer even when there is no MTP present and the peak intensity generally increases as the ratio of MTP to NTA is increased, however, after a 50% ratio, it tends to level off, if not decrease. To first order, this is indicative of the relative amount of polymer present on the surface. The dramatic increase in intensity seen from PAN-0 to PAN-25 indicates that there is a fundamental difference, from simple physisorption to strong S–Au interactions, in the adsorption processes when a thioether bearing ligand (MTP) is introduced. While this general trend seems to hold, the graft density of MTP dictates subtle changes in the film structure, as evidenced by the fact that the amide bands of PAN-50 show the largest intensities for these bands. The fact that these intensities correlate with but do not strictly follow the films mass coverage suggests a structure sensitive organization for

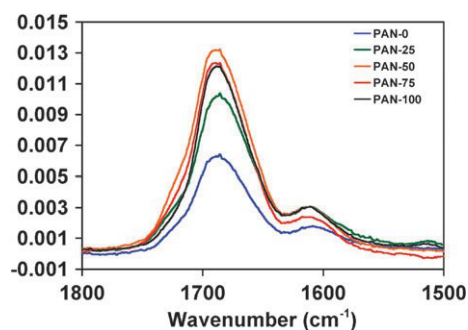


Fig. 2 RAIRS spectrum of the amide bands of modified thin films: Black-PAN-100, Red-PAN-75, Orange-PAN-50, Green-PAN-25, Blue-PAN-0.

surface bound chains in the dry state interrogated by RAIRS, one that must affect average projections of the transition dipole moments along the surface normal direction, suggesting a chain organizational structure that is responsive to the strong Au–S surface interaction.^{60–62} As these are highly hydrophilic films, it is reasonable to assume that they will form solvent penetrated structures in solutions, ones with loops and chains that extend into the aqueous bulk. We should note here that RAIRS data are collected in the absence of a liquid phase and thus reflect properties of a collapsed structure for the polymer on the surface.

In order to gain a better understanding of the adsorption dynamics of the various polymer systems and to more directly characterize them in an aqueous environment, time-dependent SPR was utilized (Fig. 3A). The adsorption of the polymer variants were followed using SPR to monitor the change in refractive index adjacent to the gold surface. These data show that the majority of the film adsorbs in less than 10 min using solutions containing 1 mg ml⁻¹ PAN. All five variants show an initial adsorption followed by a plateau region and a subsequent decline in intensity during the buffer rinse. The kinetics of film formation were measurably faster for the variants that contained some amount of MTP. In these cases, the polymer variants with little or no MTP graft density took longer to reach the plateau region indicating that the small MTP graft density inhibits film formation. Additionally, it was found that film thickness increased as a function of MTP content until 50% and then decreased as the MTP content further increased to 100%, a result consistent with the RAIRS and XPS data. The different polymer formulations showed little desorption even upon extensive washing indicating that the polymer is irreversibly bound to the surface. Ellipsometric measurements of the film thicknesses, as an independent verification, show as MTP content is increased the film thickness increases as shown in Fig. 3C.

To probe the relative protein resistance of the various polymer films to nonspecific adsorption, they were exposed to a dilute solution of BSA 30 min after film formation and then monitored *via* SPR (Fig. 3B). As a control, the adsorption of BSA onto a bare gold slide (no polymer present) shows a large initial response followed by a plateau region forming a BSA layer 3 nm thick on the surface. Relative to the pristine Au, the MTP grafted polymer surfaces all showed significant degrees of resistance to the nonspecific adsorption

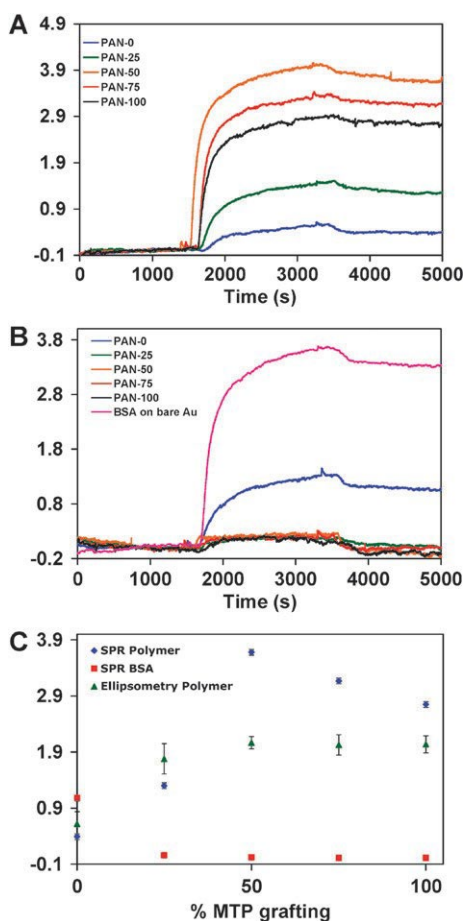


Fig. 3 SPR response of (A) modified thin films adsorbing on gold and (B) BSA adsorption profiles on polymer thin films: Black-PAN-100, Red-PAN-75, Orange-PAN-50, Green-PAN-25, Blue-PAN-0. (C) plot of thicknesses derived from SPR curves compared to the polymer thin film thicknesses as measured by ellipsometry.

of BSA. All of the MTP grafted polymers were shown to return to baseline after exposure to the BSA solutions with PAN-0 being the only polymer that showed an irreversible measurable binding response, which is consistent with the poor film quality suggested by XPS and RAIRS. It is important to note that these bifunctional grafted polymers are inherently resistant to nonspecific protein adsorption without any traditional PEG ligands present; their hydrophilic nature and strong activity as hydrogen bond acceptors suggest a very similar mechanism may operate to afford their protein resistance.^{35,36}

The ability to resist nonspecific adsorption of biomolecules is an important aspect of surfaces used to detect specific protein interactions in advanced bioassays. One specific interaction chemistry often used in metal affinity chromatography is the nickel mediated binding pair of nitrilotriacetic acid and hexahistidine. Fig. 4 shows the response of the various bifunctional polymers when exposed to concentrations of 6His tagged proteins ranging from 1 mg mL⁻¹ to 100 mg mL⁻¹ for a series of model analytes that vary markedly in mass. All three bifunctional polymer variants were tested to measure the amount of specific binding realized when using a Ni²⁺ loading. The degree of nonspecific binding was measured

in the absence of this Ni²⁺ loading. Specific binding of the human antitrypsin protein (a1-PDX 47 000 Da) to the polymer surfaces, as indicated by SPR, showed PAN-50 gave the highest amount of specific binding followed by PAN-75 then PAN-25. The PAN-50 systems also showed a small but detectable degree of nonspecific binding response (binding in the absence of Ni²⁺). Across the series it was found that, in the absence of Ni²⁺ and using the polyHis modified a1-PDX as a model, PAN-25 was the least efficient at preventing nonspecific binding, while PAN-75 was the best (Fig. 4).

To further explore how the thin films function with regards to protein adsorption and capture, we tested the binding of a

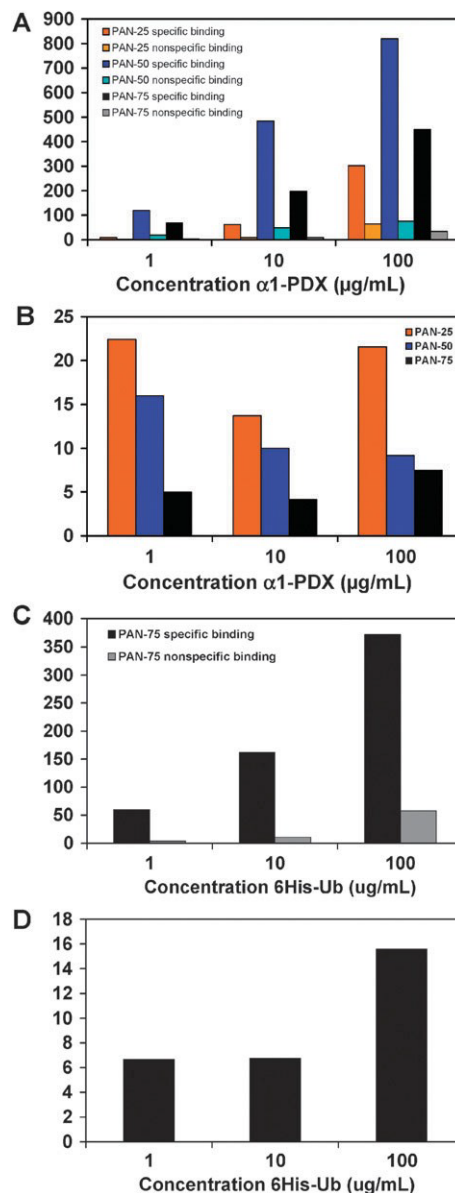


Fig. 4 A) The specific binding (Ni present) and nonspecific binding (no Ni present) of a1-PDX on the three variants (PAN-25, PAN-50 and PAN-75) of modified PAN thin films. (B) The percent nonspecific adsorption of a1-PDX relative to specific binding. (C) The specific and nonspecific binding of 6His-Ub on the PAN-75 thin film. (D) The percent nonspecific adsorption of 6His-Ub on PAN-75 relative to specific binding.

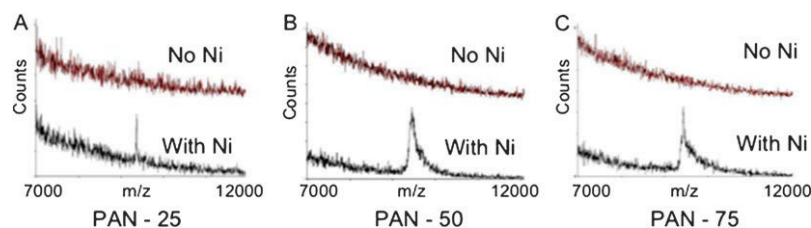


Fig. 5 MALDI-TOF mass spectra of captured 6His-Ub on (A) 1–3 MTP-NTA (B) 1–1 MTP-NTA (C) 3–1 MTP-NTA. Red traces are the response in the absence of Ni and the black traces are in the presence of Ni.

smaller protein, 6His-Ubiquitin (6His-Ub 9600 Da), at the optimal MTP graft density for promoting specific over nonspecific binding as determined in the study of α 1-PDX (PAN-75). The 6His-Ubiquitin showed slightly higher amounts of nonspecific binding than the α 1-PDX for PAN-75. While it was found that the nonspecific adsorption averaged 6% for the α 1-PDX, the nonspecific adsorption of 6His-Ub was slightly higher at 11% (Fig. 4). Taken together these data show that the structure of the film, as determined by its mass coverage (which in turn is directed by the MTP grafting) is a critical determinate of the binding and adsorption characteristics of the modified Au surfaces, where polymers with higher MTP graft densities tend to perform better as a resist towards nonspecific adsorption. Clearly many aspects of the design remain to be explored within this material class and we have done some work to briefly explore such details. First we have made PAN precursors that were much lower in molecular weight (5 000–10 000 g mol⁻¹) but with similar chemical composition of active esters. These polymers functioned poorly for the specific binding of 6His proteins although they were modestly functional as resists to the nonspecific adsorption of BSA. We also added amine functionalized PEG chains (MW 2000) to the graft solutions but found that it did little to improve the performance. We believe it remains an opportunity and need to further explore such aspects of the chemistry.

We further explored a non SPR method to determine the specific binding of 6His tagged proteins to the polymer thin films using polymer capped nanoparticles to capture 6His-Ub for analysis by MALDI (Fig. 5). Similar to the case of the flat gold surface, the polymer capping is driven by the formation of S–Au bonds and the resulting films protect the particles from aggregation, making simple washing *via* centrifugation possible. The initial capping of the NPs results in a small red shift in the plasmon adsorption that is consistent with adsorption of a thin polymer film of higher refractive index than the aqueous solution; subsequent centrifugation steps do not lead to further red shifts, strongly suggesting stabilization due to complete coating of individual particles. Capping the NPs with the bifunctional polymers provides a second independent method to examine efficacies for specific binding *via* the Ni–NTA moiety. The three variants tested (PAN-25, PAN-50, and PAN-75) all showed signal from the 6His-Ub in the presence of Ni²⁺. More significantly, no signal was observed when Ni²⁺ was not present. As shown in Fig. 5, all three polymer variants (PAN-25, PAN-50, and PAN-75) show signals from the 6His-Ub when Ni²⁺ is present and a lack of signal when it has been omitted from the NP solutions.

In this case, the MALDI data provides a diagnostic means to speciate specific capture of an analyte.

Conclusion

We describe polymer adsorbates that can be used to assemble functional thin organic films on a gold surface through S–Au bonds. The structure and function of the polyacrylamide-co-polymer thin films are determined largely by the relative graft density of a side chain thioether ligand. The dependence of the properties on the graft density indicates a hydrated, high mass coverage organization at the surface is critical for a polyacrylamide based polymer to adequately resist nonspecific protein adsorption. The inherent resistance to nonspecific protein adsorption observed in these polymer films is achieved without PEG based ligands and represent a possible new class of broadly tuned protein resists that exploit NHS based coupling reactions with ligands to provide a facile route to the formation of functionalized polymer thin films. As one example, the binding of 6His tagged proteins demonstrates this polymer system as capable of effectively resisting nonspecific adsorption of proteins, while simultaneously being highly sensitive to specific binding with potential for use in biosensing applications.

Acknowledgements

The authors would like to thank Rick Haasch for his help with the XPS data acquisition and analysis. This work was supported by the National Science Foundation (CHE0704153) and was carried out in part in the Frederick Seitz Materials Research Laboratory Central Facilities, University of Illinois, which are partially supported by the US Department of Energy under grants DE-FG02-07ER46453 and DE-FG02-07ER46471.

References

- 1 D. J. Vanderah, M. L. Walker, M. A. Rocco and K. A. Rubinson, *Langmuir*, 2008, 24, 826–829.
- 2 Y. Chang, S. Liao, A. Higuchi, R. Ruaan, C. Chu and W. Chen, *Langmuir*, 2008, 24, 5453–5458.
- 3 D. G. Castner and B. D. Ratner, *Surf. Sci.*, 2002, 500, 28–60.
- 4 D. A. Barrett, M. S. Hartshorne, M. A. Hussain, P. N. Shaw and M. C. Davies, *Anal. Chem.*, 2001, 73, 5232–5239.
- 5 R. G. Chapman, E. Ostuni, M. N. Liang, G. Meluleni, E. Kim, L. Yan, G. Pier, H. S. Warren and G. M. Whitesides, *Langmuir*, 2001, 17, 1225–1233.
- 6 W. Senaratne, L. Andruzzi and C. K. Ober, *Biomacromolecules*, 2005, 6, 2427–2448.
- 7 J. J. Gray, *Curr. Opin. Struct. Biol.*, 2004, 14, 110–115.

-
- 8 K. Y. Suh, A. Khademhosseini, J. Yang, G. Eng and R. Langer, *Adv. Mater.*, 2004, 16, 584–588.
 - 9 J. C. Love, L. A. Estroff, J. K. Kriebel, R. G. Nuzzo and G. M. Whitesides, *Chem. Rev.*, 2005, 105, 1103–1170.
 - 10 D. M. Basalyga and R. A. L. Jr, *J. Biomed. Mater. Res.*, 2003, 64a, 120–130.
 - 11 V. Silin, H. Weetall and D. J. Vanderah, *J. Colloid Interface Sci.*, 1997, 185, 94–103.
 - 12 M. M. A. Sekar, P. D. Hampton, T. Buranda and G. P. Lopez, *J. Am. Chem. Soc.*, 1999, 121, 5135–5141.
 - 13 D. R. Davies, E. A. Padlan and S. Sheriff, *Annu. Rev. Biochem.*, 1990, 59, 439–473.
 - 14 A. Pollak, H. Blumenfeld, M. Wax, R. L. Baughn and G. M. Whitesides, *J. Am. Chem. Soc.*, 1980, 102, 6324–6336.
 - 15 K. Kuroda, M. Kato, J. Mima and M. Ueda, *Appl. Microbiol. Biotechnol.*, 2006, 71, 127–136.
 - 16 G. B. Sigal, C. Bamdad, A. Barberis, J. Strominger and G. M. Whitesides, *Anal. Chem.*, 1996, 68, 490–497.
 - 17 S. H. Kim, M. Jeyakumar and J. A. Katzenellenbogen, *J. Am. Chem. Soc.*, 2007, 129, 13254–13264.
 - 18 G. J. Wegner, H. J. Lee, G. Marriott and R. M. Corn, *Anal. Chem.*, 2003, 75, 4740–4746.
 - 19 J. N. Hanson, M. J. Motala, M. L. Heien, M. Gillette, J. Sweedler and R. G. Nuzzo, *Lab Chip*, 2009, 9, 122–131.
 - 20 F. Cheng, L. J. Gamble and D. G. Castner, *Anal. Chem.*, 2008, 80, 2564–2573.
 - 21 R. A. Graff, T. M. Swanson and M. S. Strano, *Chem. Mater.*, 2008, 20, 1824–1829.
 - 22 J. Kim, H. Park, J. Kim, J. Ryu, D. Y. Kwon, R. Grailhe and R. Song, *Chem. Commun.*, 2008, 1910–1912.
 - 23 F. Khan, M. He and M. J. Taussig, *Anal. Chem.*, 2006, 78, 3072–3079.
 - 24 Y. Li, Y. Lin, P. Tsai, C. Chen, W. Chen and Y. Chen, *Anal. Chem.*, 2007, 79, 7519–7525.
 - 25 R. Valiokas, G. Klenkar, A. Tinazli, A. Reichel, R. Tampe, J. Piehler and B. Liedberg, *Langmuir*, 2008, 24, 4959–4967.
 - 26 O. Du Roure, C. Debiemme-Chouvy, J. Malthete and P. Silberzan, *Langmuir*, 2003, 19, 4138–4143.
 - 27 J. F. Hainfeld, W. Liu, C. M. R. Halsey, P. Freimuth and R. D. Powell, *J. Struct. Biol.*, 1999, 127, 185–198.
 - 28 J. Schmitt, H. Hess and H. G. Stunnenberg, *Mol. Biol. Rep.*, 1993, 18, 223–230.
 - 29 S. Herrwerth, W. Eck, S. Reinhardt and M. Grunze, *J. Am. Chem. Soc.*, 2003, 125, 9359–9366.
 - 30 M. Mrksich and G. M. Whitesides, *Annu. Rev. Biophys. Biomol. Struct.*, 1996, 25, 55–78.
 - 31 E. Ostuni, L. Yan and G. M. Whitesides, *Colloids Surf., B*, 1999, 15, 3–30.
 - 32 R. G. Chapman, E. Ostuni, L. Yan and G. M. Whitesides, *Langmuir*, 2000, 16, 6927–6936.
 - 33 D. J. Vanderah, G. Valincius and C. W. Meuse, *Langmuir*, 2002, 18, 4674–4680.
 - 34 R. L. C. Wang, H. J. Kreuzer and M. Grunze, *J. Phys. Chem. B*, 1997, 101, 9767–9773.
 - 35 E. Ostuni, R. G. Chapman, R. E. Holmlin, S. Takayama and G. M. Whitesides, *Langmuir*, 2001, 17, 5605–5620.
 - 36 E. Ostuni, B. A. Grzybowski, M. Mrksich, C. S. Roberts and G. M. Whitesides, *Langmuir*, 2003, 19, 1861–1872.
 - 37 N. A. Alcantar, E. S. Aydil and J. N. Israelachvili, *J. Biomed. Mater. Res.*, 2000, 51, 343–351.
 - 38 F. Sun, D. G. Castner, G. Mao, W. Wang, P. McKeown and D. W. Grainger, *J. Am. Chem. Soc.*, 1996, 118, 1856–1866.
 - 39 G. Zhen, D. Falconnet, E. Kuennemann, J. V. o'fo's, N. Spencer, M. Textor and S. Zürcher, *Adv. Funct. Mater.*, 2006, 16, 243–251.
 - 40 C. D. Bain and G. M. Whitesides, *Science*, 1988, 240, 62–63.
 - 41 J. Zhou, J. Ralston, R. Sedev and D. A. Beattie, *J. Colloid Interface Sci.*, 2009, 331, 251–262.
 - 42 S. Lal, N. K. Grady, J. Kundu, C. S. Levin, J. B. Lassiter and N. J. Halas, *Chem. Soc. Rev.*, 2008, 37, 898–911.
 - 43 I. Tokareva, S. Minko, J. H. Fendler and E. Hutter, *J. Am. Chem. Soc.*, 2004, 126, 15950–15951.
 - 44 C. J. Murphy, T. K. Sau, A. M. Gole, C. J. Orendorff, J. Gao, L. Gou, S. E. Hunyadi and T. Li, *J. Phys. Chem. B*, 2005, 109, 13857–13870.
 - 45 S. Link and M. A. El-Sayed, *J. Phys. Chem. B*, 1999, 103, 4212–4217.
 - 46 A. W. H. Lin, N. A. Lewinski, J. L. West, N. J. Halas and R. A. Drezek, *J. Biomed. Opt.*, 2005, 10, 064035–10.
 - 47 S. Mornet, S. Vasseur, F. Grasset and E. Duguet, *J. Mater. Chem.*, 2004, 14, 2161–2175.
 - 48 Z. Wang, R. Levy, D. G. Fernig and M. Brust, *J. Am. Chem. Soc.*, 2006, 128, 2214–2215.
 - 49 J. S. Kirk and P. W. Bohn, *J. Am. Chem. Soc.*, 2004, 126, 5920–5926.
 - 50 A. J. Haes, S. Zou, G. C. Schatz and R. P. Van Duyne, *J. Phys. Chem. B*, 2004, 108, 6961–6968.
 - 51 G. Schneider, G. Decher, N. Nerambourg, R. Praho, M. H. V. Werts and M. Blanchard-Desce, *Nano Lett.*, 2006, 6, 530–536.
 - 52 C. J. Murphy, A. M. Gole, J. W. Stone, P. N. Sisco, A. M. Alkilany, E. C. Goldsmith and S. C. Baxter, *Acc. Chem. Res.*, 2008, 41, 1721–1730.
 - 53 J. Kneipp, in *Surface-Enhanced Raman Scattering*, 2006, pp. 335–349.
 - 54 A. W. Wark, H. J. Lee, A. J. Qavi and R. M. Corn, *Anal. Chem.*, 2007, 79, 6697–6701.
 - 55 F. D'Agosto, M. Charreyre, F. Me'is, B. Mandrand and C. Pichot, *J. Appl. Polym. Sci.*, 2003, 88, 1808–1816.
 - 56 J. Turkevich, P. C. Stevenson and J. Hillier, *Discuss. Faraday Soc.*, 1951, 11, 55–75.
 - 57 E. Kretschmann and H. Raether, *Z. Naturforsch., Teil A*, 1968, 23, 2135.
 - 58 L. S. Jung, C. T. Campbell, T. M. Chinowsky, M. N. Mar and S. S. Yee, *Langmuir*, 1998, 14, 5636–5648.
 - 59 N. H. Mack, R. Dong and R. G. Nuzzo, *J. Am. Chem. Soc.*, 2006, 128, 7871–7881.
 - 60 K. R. Finnie, R. Haasch and R. G. Nuzzo, *Langmuir*, 2000, 16, 6968–6976.
 - 61 A. R. Noble-Luginbuhl and R. G. Nuzzo, *Langmuir*, 2001, 17, 3937–3944.
 - 62 C. Bubeck and D. Holtkamp, *Adv. Mater.*, 1991, 3, 32–38.
-